Title: Quantitative structure-activity relationship analysis of substituted arylazo pyridone dyes in photocatalytic system: Experimental and theoretical study

Author: J. Dostanić D. Lončarević M. Zlatar F. Vlahović D.M. Jovanović

PII: S0304-3894(16)30445-9
DOI: http://dx.doi.org/doi:10.1016/j.jhazmat.2016.05.015
Reference: HAZMAT 17703

To appear in: *Journal of Hazardous Materials*

Received date: 9-2-2016
Revised date: 17-4-2016
Accepted date: 4-5-2016

Please cite this article as: J.Dostanić, D.Lončarević, M.Zlatar, F.Vlahović, D.M.Jovanović, Quantitative structure-activity relationship analysis of substituted arylazo pyridone dyes in photocatalytic system: Experimental and theoretical study, Journal of Hazardous Materials http://dx.doi.org/10.1016/j.jhazmat.2016.05.015

Quantitative structure-activity relationship analysis of substituted arylazo pyridone dyes in photocatalytic system: Experimental and theoretical study

J. Dostanić[a, *], D. Lončarević[a], M. Zlatar[b], F. Vlahović[c], D.M. Jovanović[a]

[a] *University of Belgrade, Institute of Chemistry, Technology and Metallurgy, Department of Catalysis and Chemical Engineering, Njegoševa 12, 11000 Belgrade, Serbia*

[b] *University of Belgrade, Institute of Chemistry, Technology and Metallurgy, Department of Chemistry, Njegoševa 12, 11000 Belgrade, Serbia*

[c] *University of Belgrade, Innovation center of the Faculty of Chemistry,11000 Belgrade, Serbia*

[*] Corresponding author. Tel: +381 11 2630 213; fax: +381 11 2637 977;
E-mail address: jasmina@nanosys.ihtm.bg.ac.rs (J. Dostanić).

Graphical abstract

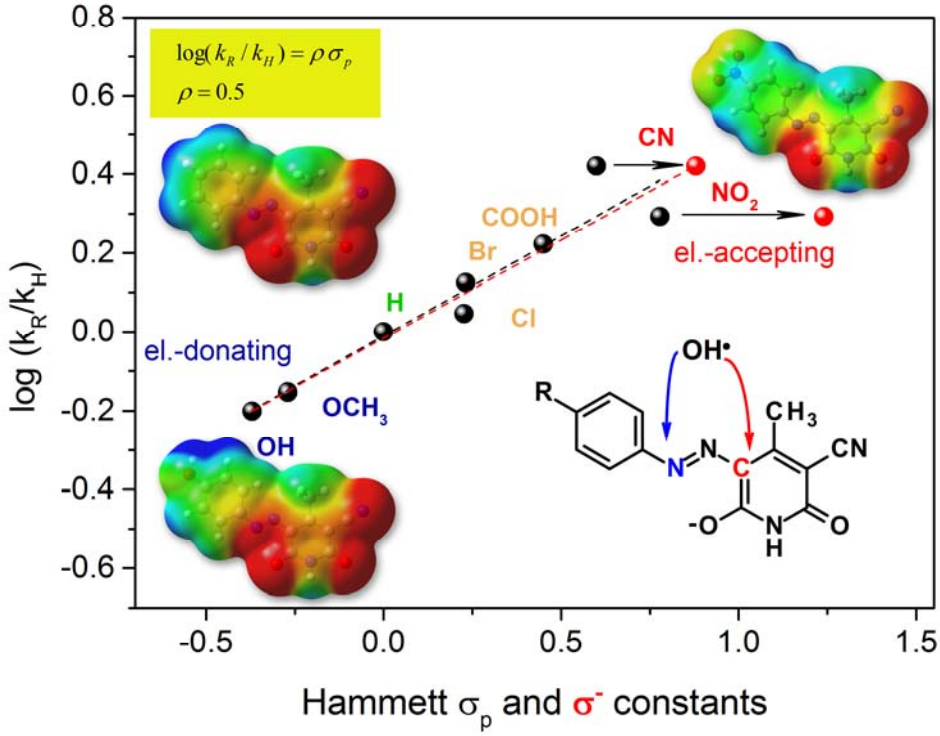

Highlights:

- Electronic effects of *para* substituted arylazo pyridone dyes.
- Linear relationship between Hammett σ_p constants and dyes photoreactivity.
- The photocatalytic reactions facilitated by el.-acceptors and retarded by el.-donors.
- Fukui functions to analyze the reactivity on concurrent sites within a molecule.
- Hydroxyl radicals sustain attack from two reaction sites, depending on a substituent type.

Abstract

A series of arylazo pyridone dyes was synthesized by changing the type of the substituent group in the diazo moiety, ranging from strong electron-donating to strong electron-withdrawing groups. The structural and electronic properties of the investigated dyes was calculated at the M062X/6-31+G(d,p) level of theory. The observed good linear correlations between atomic charges and Hammett σ_p constants provided a basis to discuss the transmission of electronic substituent effects through a dye framework. The reactivity of synthesized dyes was tested through their decolorization efficiency in TiO_2 photocatalytic system (Degussa P-25). Quantitative structure-activity relationship analysis revealed a strong correlation between reactivity of investigated dyes and Hammett substituent constants. The reaction was facilitated by electron-withdrawing groups, and retarded by electron-donating ones. Quantum mechanical calculations was used in order to describe the mechanism of the photocatalytic oxidation reactions of investigated dyes and interpret their reactivities within the framework of the Density Functional Theory (DFT). According to DFT based reactivity descriptors, i.e. Fukui functions and local softness, the active site moves from azo nitrogen atom linked to benzene ring to pyridone carbon atom linked to azo bond, going from dyes with electron-donating groups to dyes with electron-withdrawing groups.

Keywords: arylazo pyridone dyes, substituent effect, photocatalysis, Hammett equation, DFT-*ab initio* calculations, Fukui functions.

1. INTRODUCTION

Azo dyes containing heterocyclic pyridone ring have recently attracted the interest of many research groups due to their higher tinctorial strength, brighter dyeing and excellent light, washing and sublimation fastness, and chromophoric strength in relation to azo dyes based uniquely on azobenzene derivatives [1]. The heterocyclic azo dyes are generally used as disperse dyes, suitable for dying polyester fabrics [2]. Due to inefficiencies of the industrial dyeing process, about 10-15% of the dyes are lost in the effluent during their synthesis and dyeing processes [3]. Such excessive discharge of the dye effluents can lead to severe contamination of surface and ground water, hence affecting aquatic life, especially in the vicinity of dyeing industries [4, 5]. Azo dyes are of special environmental concern since anaerobic degradation of these dyes leads to the generation of highly toxic and carcinogenic aromatic intermediate products (e.g. aromatic amines) [6]. Therefore, the removal of the dyes from wastewater is gaining great importance, particularly as new regulations on industrial effluent discharges are being enforced.

Among different available methods used for wastewater treatment, photocatalytic processes, have an advantage being safe, effective, economic, and environmentally friendly processes. The photocatalytic reactions occur, at least principally, in the adsorbed phase, and include OH radical or $O_2^{\bullet-}$ attack on pollutant adsorbed onto the surface of the catalyst [7]. Thereby, the catalyst surface and the nature of organic substances to be degraded are one of the crucial parameters determining the photodegradation rate. A numerous studies have shown that the reactivity of aromatic compounds can be drastically affected by the electronic nature of substituent group in the aromatic ring [8, 9]. The Hammett substituent constants, which quantify the electron withdrawing or donating capabilities of a given substituent, have been successfully applied in various research areas to obtain a quantitative description of

many chemical equilibriums and reactions [10, 11]. Mazzile et al. [12] showed that reactivity of *para*-substituted phenols via photo-assisted Fenton catalysis increases with increased electronic density of the aromatic ring. The structural effect of *para* substituted phenols on their photoreactivity via TiO_2 catalysis is studied in the work of Parra et al. [13]. The results from this study demonstrated a clear correlation between degradation rate data and Hammett constants for the majority of investigated phenols. The photodecomposition of various amino acids onto TiO_2 aqueous suspension was examined using Hammett correlations to gain insight on the mechanism of photooxidation [14].

In the recent years, theoretical investigations have been extensively performed to provide important information about reaction pathways [15-18]. DFT-based reactivity descriptors, such as Fukui functions and local softness, [19] were widely used to predict the most probable reactive sites without actual calculations of the corresponding potential energy surface [20, 21].

Our recently published paper investigated the substituent effects on the absorption spectra and acid-base and tautomeric equilibrium of the synthesized 5-(4-substituted arylazo)-6-hydroxy-4-methyl-3-cyano-2-pyridones using Hammett's equation [22]. The present study extends the previous investigation with the aim to obtain the quantitative description of the electronic substituent effects on the atomic charges and photocatalytic properties of the selected dyes. The primary attack of photogenerated hydroxyl radicals on dye compound was applied as reaction model for determination of photocatalytic reactivity of investigated dyes. DFT based reactivity descriptors, e.g. condensed Fukui function and local softness were used to describe the mechanism of the photocatalytic oxidation reactions by predicting the preferred site of hydroxyl radical attack.

2. EXPERIMENTAL

2.1. Synthesis and structure of arylazo pyridone dyes

The synthesized arylazo pyridone dyes, 5-(4-substituted arylazo)-6-hydroxy-4-methyl-3-cyano-2-pyridones belong to a group of heterocyclic azo dye compounds (Scheme 1). The investigated dyes possess the same benzene/pyridone skeleton with different substituent group (R) in the benzene ring. The synthesis and characterization of investigated dye molecules (compounds) were reported in our previously published papers [23, 24].

2.2. Photocatalytic activity studies

The photocatalytic degradation of investigated dyes was performed in an open cylindrical thermostated Pyrex cell of a 1 L capacity. A commercially available TiO_2, Aeroxide P25, Evonik Degussa GmbH (80 % anatase - 20% rutile, surface area - 52 m^2 g^{-1}, mean diameter - approximately 30 nm) was used as a photocatalyst. The irradiation was performed using Osram Vitalux lamp, with a power consumption of 300 W, housed 50 cm above the top surface of the dye solution. The emission spectrum of the used lamp simulates solar irradiation.

Prior to illumination, the dye suspensions were magnetically stirred in the dark for 30 min in order to achieve adsorption-desorption equilibrium.

The initial pH of the suspension was adjusted to 12 using sodium hydroxide solution. The tests were performed in alkaline media in order to increase dye solubility to overcome the effects of substituent anionic group on adsorption (eg. -COOH group becomes negatively

charged at lower pH). The mass of the used TiO_2 was 0.5 g; the concentration of dye solution was $1x10^{-5}$ mol/dm^3; the volume of the dye solution was 500 mL.

During irradiation, the aliquots were taken periodically, and the concentration of the dyes was followed using UV-Vis spectrophotometer (Thermo Electron Nicolet Evolution 500). The concentration of the dyes was calculated according to absorption maxima of particular dye in the visible region [**Error! Bookmark not defined.**]. Before analysis, the aliquots were centrifuged for 10 min at the rate of 17000 rpm. The photodegradation kinetics was analyzed in terms of simplified Langmuir-Hinshelwood model (Eq. 1). Apparent first order rate constant k_{app} (min^{-1}) was determined for each test and used as a measure of the photocatalytic efficiency.

$$\ln(C / C_0) = k_{app}\, t \qquad (1)$$

where C is dye concentration at irradiation time t and C_0 is initial dye concentration (at zero irradiation), both given in mol/dm^3.

2.3. Quantum chemical calculations

The quantum chemical calculations have been carried out with Gaussian 09 electronic structure program suite (revision C.01), by using Density Functional Theory approach (DFT) [25]. The widely used and well-known M06-2X functional and 6-31+G(d,p) basis set [26-28] have been chosen for calculation of structural and electronic properties of the studied dyes. Atomic charges based on Hirshfeld analysis [29] and Natural Population Analysis (NPA) [30] as well as local reactivity indices were used to analyze the reactivity of different sites within a molecule, and to explain the reactivity differences between the investigated dyes. From the

Hard and Soft Acids and Base (HSAB) principle [31] and DFT method, it has been possible to identify many useful and important reactivity parameters, such as Fukui function (*f(r)*) [32, 33]. However, for studying the reactivity at the atomic level, a more convenient way of calculating the Fukui function is through the condensed forms of the Fukui function for an atom *j* in a molecule, which are expressed as Eqs (2-4) [34].

$$f_j^-(r) = q_{j(N-1)} - q_{j(N)}, \tag{2}$$

$$f_j^+(r) = q_{j(N)} - q_{j(N+1)}, \tag{3}$$

$$f_j^0(r) = \frac{1}{2}\{q_{j(N-1)} - q_{j(N+1)}\} \tag{4}$$

for an electrophilic ($f_j^-(r)$), nucleophilic ($f_j^+(r)$) of free radical attack ($f_j^-(r)$) on the reference molecule respectively. In these equations q_j is the atomic charge, evaluated from the Hirshfeld analysis, at the j_{th} atomic site in the neutral (*N*), anionic (*N+1*), or cationic (*N-1*) chemical species. The Fukui function contains relative information about different sites of a molecule, while the local softness s(r) is more important when comparing different sites in different molecules. The respective atomic softness parameters can be obtained by multiplying Fukui function values with global softness S, s(r) = Sf(r) [35]. In the finite difference approximation, S is calculated (Eq. 5)from the first vertical ionization energy (E_i) and electron affinity (E_{ea}) of the molecule:

$$S = \frac{1}{E_i - E_{ea}}, \tag{5}$$

3. RESULTS AND DISCUSSION

3.1. DFT atomic charges of arylazo pyridone dyes

The molecular structure of the investigated arylazo pyridone dyes is presented in Scheme 1. The photocatalytic tests were conducted in alkaline media, where dyes existed in a form of an anion, which represents "resonance hybrid" between azo anion (A) and hydrazone anion (Hy) canonical forms with a negative charge being delocalized over pyridone oxygen and azo nitrogen atom (Scheme 2).

The geometry optimizations of the investigated dyes generated reliable minima structures, as confirmed by the absence of imaginary force constants in the vibrational analysis. The geometry optimization yielded planar structure, which enabled the conjugation throughout the whole dye molecule [**Error! Bookmark not defined.**]. Table 1 presents the computed Hirshfeld atomic charges from M062X/6-31+G(d,p) calculations for pyridone oxygen, carbon and azo nitrogen atoms, obtained using Hirshfeld analysis. The numbering system used throughout the calculations is shown in Scheme 1.

Inspection of the data in Table 1 shows that the negative charge is distributed between pyridone oxygen atom and both azo nitrogen atoms. Pyridone oxygen atom bears the majority of the negative charge. It is also noticeable that atomic charges of oxygen and nitrogen atoms are affected by the type of investigated dye, i.e. the type of substituent on a phenyl ring. NPA charges give the same trend (Table S1 in the Supplementary Information). To gain better insight on the later point, Hammett's linear free energy relationship (LFER) was applied using Eq. (6).

$$G_R = G_H + \rho\sigma_p \quad (6)$$

where G_R and G_H refer to the atomic charges for substituted and unsubstituted dyes respectively. The slope of this linear correlation, ρ, represents the sensitivity of the atomic charges to the effect of substituent. σ_p represents Hammett substituent constant at the *para* position. A positive value of σ_p indicates an electron-withdrawing group, while a negative value indicates an electron-donating group. According to Eq. (5), Fig. 1 shows a plot of the atomic charges of carbon atoms linked to azo bond, pyridone oxygen and azo nitrogen atoms against Hammett σ_p constants.

As shown in Fig. 1, a good linear correlation between the Hammett σ_p constants and atomic charges of selected atoms is observed (correlation coefficients, $R^2 > 0.92$). The results revealed that substituents on the aromatic ring exert influence on electron density distribution. To quantify and compare the effect of substituents on atomic charges, the slope of the linear curves were determined according to Eq. 6. The greater the magnitude of the slope, the greater the sensitivity of atomic charge to the substituent change. The obtained slopes of the curves for C6, O1, N4, C5 and N3 were (28, 15, 11, 10 and 6)x10^{-3} min^{-1} respectively. The substituents exert the strongest influence on C6 atomic charge, since this carbon atom is nearest to the substituent group. Analysis of atomic charge sensitivity also revealed that O1 is second the most sensitive atom to the substituent effect. This result undoubtly indicates the existence of the conjugation throughout the whole dye molecule. The negative charge on the N3 nitrogen atom is not strongly affected by the substituent type.

The results also revealed that the electron density of the N4 atom increases sensitively ongoing from the dyes with electron-donating groups to the dyes with electron-withdrawing

groups, while electron density of O1 pyridone oxygen atom and carbon C5 and C6 atoms decreases. The rationale behind these findings is elaborated in the following. The negative charge on the pyridone oxygen atom and electron rich character of pyridone ring tend to strengthen the electron-accepting power of acceptors resulting in an increased resonance interaction with pyridone ring; the acceptors pull electrons from the pyridone ring to N4 atom, thus increasing the negative charge on the N4 azo nitrogen atom and decreasing negative charge on O1 pyridone oxygen atom. On the other hand, extra available electrons in pyridone ring have the tendency to weaken the donating power of substituents, which results in prevented resonance interactions between an electron donating group and pyridone ring, maintaining negative charge in the pyridone ring. The results also indicate that the negative charge on the N3 nitrogen atom is not strongly affected by the substituent type.

The above analysis of partial atomic charges is in accordance with global softness, *S*, of investigated dyes, Table 1. In fact, there is a clear linear relation between softness and Hammett σ_p constants, Fig. 2. The same is true for both E_i and E_{ea}, Table S2 and Fig. 2. Dyes with electron-donating groups are being more soft than those with electron-withdrawing substituents.

3.2. Electrostatic potential molecular surfaces

The molecular electrostatic potential (MEP) for substituted dyes are shown in Fig. 3. The MEP is related to the electronic density, and because of that it is an excellent approach for visualising chemically active sites, that potentially participate in different chemical reactions. The MEP could, therefore, be a very useful tool for determining suitable areas for electrophilic, nucleophilic, or in our case radical attacks.

The values of the electrostatic potential at the surface are shown by different colours: blue indicates the most positively charged part of the examined molecule, while red colour represents the most negatively charged part. Potential decreases in the order blue > green > yellow > orange > red. The plot of the electrostatic potential mapped onto the electron density surface is modelled in the colour range from -0.0190 a.u. to 0.0400 a.u.

In Fig. 3 the MEP maps of presented dye molecules in neutral and anionic form are presented. As can be seen, the distribution of negative charge in anionic form (Fig. 3a) is located in the part of a molecule between pyridone oxygen and azo bond, while this distribution is absent in protonated form (Fig. 3b). In protonated form, the negative charge is equally distributed over carbon atoms of the benzene ring. In anionic form, decreased electron density on the benzene ring is due to the electron withdrawal from benzene ring to pyridone ring.

Electron distribution in the molecules varies depending on the characteristics of the substituent on the aromatic ring. In the case of dyes with the electron-donating hydroxyl group (Fig. 3c) the presence of electron distribution spreads from oxygen O1 atom to nitrogen atoms. This area in dye substituted with the nitro group (Fig. 3d) is more deficit in electron density, since the electrons are withdrawn from the pyridone ring to NO_2 group. Additionally, carbon atoms of benzene ring bonded to the electron-donating OH group are more electron-deficient compared to the benzene carbon atoms of dye with NO_2 group, due to a stronger resonance interaction in the later compound.

3.3. Photocatalytic degradation of arylazo pyridone dyes-Hammett study

Before examining photocatalytic degradation of the synthesized dyes, two control experiments were performed: (i) dye removal in the dark in the presence of TiO_2 (1.0 g L^{-1})

and (ii) dye degradation under simulated sunlight in the absence of TiO_2 (photolysis). The concentration of dye in both experiments was $1x10^{-5}$ mol/L. The adsorption of anionic form of the dyes was below the level of spectroscopic accuracy measurement, so we did not detect adsorption in ordinary experiment setup. In addition, the photolysis of the dyes was not detected. The results from these control tests indicate that both TiO_2 and UV were necessary for effective degradation of the tested dyes.

The major benefit of low adsorption is that adsorption constant in Langmuir-Hinshelwood model becomes negligible and reaction kinetics can be simplified to reduced Langmuir-Hinshelwood; thus the reaction between hydroxyl radical and anionic dye becomes a phase that determines the reaction rate. Therefore, such reaction conditions provide a straightforward way to study substituent effect on the reaction mechanism and on the reaction rate constants.

Time-dependent photodegradation efficiency of the investigated dyes is presented in Fig. 4. The apparent first order rate constant k_{app} (min^{-1}) was determined from observed kinetic curves using simplified Langmuir-Hinshelwood model and presented in Table 1.

The obtained results clearly show that photocatalytic reaction rate is strongly affected by the type of the phenyl substituent group. For the quantitative assessment of the substituent effects on the reaction rate, LFER model, based on simple Hammett equation was applied (Eq. 7):

$$\log(k_R / k_H) = \rho \sigma_p \qquad (7)$$

The slope of linear correlation is the reaction constant, ρ, reflecting the sensitivity of reaction rate to the substituent effects. The positive sign of ρ implies the development of a negative charge at the reaction site during the formation of the transition state in the rate determining step, and vice versa. Apparent first order rate constant k_R refers to the substituted dye, while k_H refers to the unsubstituted dye. According to Eq. (6), Fig. 5 shows a plot of the first term against σ_p.

Hammett correlation $\log(k/k_0)$ vs. σ_p reveals that the electron-withdrawing groups enhance, while electron-donating groups retard the reaction rate compared to the unsubstituted dye. This is in accordance with HSAB principle, and the linear relationship between S and σ_p (Fig. 2). Although plot $\log(k/k_0)$ vs. σ_p shows generally a good correlation (R^2=0.90), some points are markedly of the line (CN and NO_2). Deviation of CN and NO_2 data points from the fitted line could be explained with extra resonance interaction between the substituent and the reaction site, i.e. through conjugation. It has been found that reactions involving through conjugations correlate better with σ^- or σ^+ Hammett constants than with Hammett σ_p constants [37]. In the case of CN substituent, plotting $\log(k/k_0)$ versus σ^- constants (σ^-=0.88) [**Error! Bookmark not defined.**] gave better Hammett correlation (R^2=0.98) (Fig. 2, open squares) than it does with the original Hammett σ_p constants (Fig. 2, closed squares). However, by using σ^- constants for NO_2 substituent (σ^-=1.24) [**Error! Bookmark not defined.**], a higher deviation from the straight line is obtained, indicating possible change of reaction mechanism. It has been suggested that the mechanism of the photodegradation of azo compounds under UV-visible light illumination is usually initiated by hydroxyl radical attack on either the carbon atom bearing the azo linkage or on the azo nitrogen atoms. Due to the electrophilic character of the hydroxyl radical, it can be expected

that photocatalytic reactions are favoured by increased electron density at the reaction site, i.e. accelerated by electron-donating substituents, and retarded by electron-withdrawing ones. Indeed, the latter has been confirmed in various works [**Error! Bookmark not defined.**, **Error! Bookmark not defined.**]. Most of these papers investigate simple organic compounds, consisted of an aromatic ring with only one possible reaction site. Conversely, the investigations in this study reveal that the photocatalytic degradation of arylazo pyridone dyes is being inhibited by the electron-donating groups and accelerated by electron-withdrawing one with respect to unsubstituted dye (Fig. 2) and the positive Hammett reaction constant was obtained (ρ=0.507). The positive sign of ρ implies the development of a negative charge (or the disappearance of a positive charge) at the reaction site during the formation of the transition state in the rate determining step. In order to explain the result obtained, it should first be noted that, investigated dyes in this study were in the form of an anion, with increased amount of negative charge. The development of a negative charge at the reaction site during the formation of the transition state is most likely a consequence of the movement of negative charge from pyridone oxygen to a reaction site, leading to the positive Hammett constant.

Recent works investigating more simple compounds, such as substituted phenols, imply that the electronic effects of substituents may be unobstructedly transmitted through the benzene ring, and the electronic density at the reaction site is primarily influenced by the type of substituent in benzene ring [**Error! Bookmark not defined.**]. In the present work, a series of more complex compounds, 5-(4-substituted arylazo)-6-hydroxy-4-methyl-3-cyano-2-pyridones, is studied, where the *para* substituted benzene ring is linked to the azo bond bearing heteroaromatic ring. In such complex structures, charge on a reactive site is influenced, not only by the substituent group, but also by the interaction between aromatic and heteroaromatic (pyridone) ring. Therefore, the application of simple Hammett equation

would not be sufficient for a complete understanding of the reaction mechanism, but rather additional analysis comprising molecular descriptors ought to be conducted.

3.4. Fukui functions as site reactivity descriptors for predicting dye photoreactivity

Hydroxyl radicals, either adsorbed or present in the bulk solution, are generally considered to be the principle reactive species responsible for the photocatalytic reaction. Therefore, the model reaction used in the theoretical part of this study is based on the primary attack of the photogenerated OH radicals on dye substrate [38]. Due to a strong electrophilic character of the hydroxyl radicals, it can be expected that hydroxyl radicals would attack the region with the highest electron density.

According to the results of DFT calculations, the N4 nitrogen atom carries the most negative charge (Table 1), representing the most electron-populated part of the dye. The negative charge on the N4 atom increases when going from dyes with electron-donating substituents to dyes with electron-withdrawing substituents in the same direction as a reaction rate, suggesting this to be the likely point of attack by OH radical. However, the use of partial charges for prediction of the reaction site may produce some contradicting conclusions when larger molecules are investigated. In these cases, it is preferable to use the local reactivity indices, e.g. the Fukui functions, instead of the electronic density, to predict the possible reactive site. In fact, Fukui function (f) and local softness have already been applied to a wide range of chemical problems, such as to study solute-solvent interactions [39, 40], stabilization of different tautomeric forms [41] and also to predict the reaction mechanisms of many types of reactions [42-44].

Table 2 list the values of condensed radical Fukui functions and local softness, in terms of Hirshfeld charges, computed for azo nitrogen atoms and carbon atoms linked to azo

bond. Table S3 reports the condensed radical Fukui functions and local softness calculated from NPA charges. In order to obtain the best reactivity descriptor and the nature of the photocatalytic oxidation reactions of the substituted arylazo pyridone dyes, "softness-matching principle" [45] was used. This principle is based on HSAB principle. According to the local HSAB principle, soft atoms react preferentially with other soft atoms and hard atoms with other hard atoms. For these reactions the difference between the oxygen atom of the attacking OH radical and the atom of arylazo pyridone dye (C5, N3, N4 or C6) that may undergo the radical attack was calculated for each of the investigated molecules. On inspection of the results presented in Table 2, it is conclusive that the hydroxyl radicals sustain attack from two reaction sites, depending on a dye employed. The attack occurs at the N4 nitrogen atom for all substituted dyes, except the one with NO_2 substituent, that would sustain the attack on C5 carbon atom, linked to the pyridone ring. It follows that photocatalytic degradation of dye containing NO_2 substituent proceeds through mechanism pathway, that differs from the ones of other dyes. These results explain our previous experimental finding, which revealed that only a dye compound that contains NO_2 substituent deviates from Hammett correlation (Fig. 5). Maximal local reactivity indices, i.e. Fukui functions and local softness on N4 (for dyes with R=OH, OCH_3, H, Cl, Br, COOH and CN) and on C5 (for R=NO_2) are linearly related to the $\log(k/k_0)$, Fig. 6 (R^2=0.92 and R^2=0.93 respectively). The obtained results clearly demonstrate the power of the Hammett correlation, especially when accompanied with DFT calculations.

4. CONCLUSION

In this study, the effect of substituent in phenyl ring on the electronic properties and photocatalytic decomposition of synthesized 5-(4-substituted arylazo)-6-hydroxy-4-methyl-3-

cyano-2-pyridones was studied. The results showed that electron distribution in the dye molecules varies depending on the characteristics of the substituent on the aromatic ring.
The calculated atomic charges of azo nitrogen atoms and pyridone oxygen correlates well with Hammett σ_p constants, implying existence of resonance interactions between aromatic and heterocyclic ring.

The photocatalytic degradation of substituted dyes was performed using TiO_2 in a basic media, under simulated solar irradiation. Experimentally obtained reaction rate constants were correlated with simple Hammett equation. The results showed that the reaction rate was inhibited by electron-donating substituents, and enhanced by electron-withdrawing ones. The development of a negative charge at the reaction site during the formation of the transition state is most likely a consequence of movement of negative charge from pyridone oxygen to reaction site. A better Hammett correlation is obtained by using the values of σ^- for strong electron releasing substituent rather than those of σ_p, thus indicating the extent of resonance interactions between substituent group and reaction site. The facts that investigated dyes have complex structure, with more than one possible reactive site and that NO_2 substituted dye does not show good correlation, even using the corrected σ^- Hammett constant, indicate possible change in mechanism pathway.

Quantum mechanical calculations were used in order to describe the initial mechanism of the photocatalytic oxidation reactions of arylazo pyridone dyes and to reveal mechanism changeover within the framework of the DFT. The reaction model used in the computational part of this study is the reaction between the arylazo pyridone dye and the photogenerated hydroxyl radicals. According to Fukui functions and local softness the hydroxyl radical attack preferentially occurs at the N4 nitrogen atom for all dyes except the one with NO_2 substituent that sustains the attack on C5 carbon atom. The obtained calculations were used as a starting point for understanding the degradation mechanism of mentioned arylazo pyridone dyes. A

more detailed insight into the reaction mechanism would be provided by calculating the potential energy surfaces of the tested photocatalytic reactions. This complex task is planned to be the subject of our further investigation.

Acknowledgments:

This work was supported by the Ministry of Education, Science and Technological Development of the Republic of Serbia (Project No. III 45001).

References

[1] Božić, B., Alimmari, A.S., Mijin, D.Ž., Valentić, N.V., Uščumlić G.S., 2014. Synthesis, structure and solvatochromic properties of novel dyes derived from 4-(4-nitrophenyl)-3-cyano-2-pyridone. J. Mol. Liq. 196, 61-68.

[2] Chen, C.C., Wang, I.J., 1991. Synthesis of some pyridone azo dyes from 1-substituted 2-hydroxy-6-pyridone derivates and their colour assessment. Dyes Pigments. 15, 69-82.

[3] Baban, A., Yediler, A., Lienert, D., Kemerdere, N., Kettrup, A., 2003. Ozonation of high strength segregated effluents from a woollen textile dyeing and finishing plant. Dyes Pigments. 58, 93-98.

[4] O'Neill, C., Hawkes, F.R., Hawkes, D.L., Lourenyo, N.D., Pinheiro, H.M., Delee, W., 1999. Colour in textile effiuents-sources, measurement, discharge consents and simulation: a review. J. Chem. Technol. Biotechnol. 74, 1009-1018.

[5] Pinheiro, H.M., Touraud, E., Thomas, O., Meding, B., Belin, L., 2004. Aromatic amines from azo dye reduction: status review with emphasis on direct UV spectrophotometric detection in textile industry wastewaters. Dyes Pigments. 61, 121-139.

[6] Nilsson, R., Nordlinder, R., Wass, U., 1993. Asthma, rhinitis, and dermatitis in workers exposed to reactive dyes. Brit. J. Ind. Med. 50, 65-70.

[7] Kaneko, M., Okura, I., 2002. Fundamental Aspects of Photocatalysts. Photocatalysis Science and Technology, first ed., Kodansha Ltd, Tokyo.

[8] Bhuvaneshwari, D.S., Elango, K.P., 2008. Solvent hydrogen bonding and structural effects on nucleophilic substitution reactions: Part 4 - Reaction of 2-chloro-5-nitropyridine with para-substituted anilines in acetonitrile/dimethylformamide mixtures. J. Mol. Liq. 143, 147-153.

[9] Huang, X., Feng, Y., Hu, C., Xiao, X., Yu, D., Zou, X., 2015. Mechanistic QSAR models for interpreting degradation rates of sulfonamides in UV-photocatalysis systems. Chemosphere. 138, 183-189.

[10] Hammett, P., 1935. Some relations between reaction rates and equilibrium constants. Chem. Rev. 17, 125-136.

[11] Hammett, L.P., 1937. The effect of structure upon the reactions of organic compounds. Benzene derivatives. J. Am. Chem. Soc. 59, 96-103.

[12] Mazille, F., Schoettl, T., Lopez, A., Pulgarin, C., 2010. Physico-chemical properties and photo-reactivity relationship for para-substituted phenols in photo-assisted Fenton system. J. Photochem. Photobiol., A. 210, 193-199.

[13] Parra, S., Olivero, J., Pacheco, L., Pulgarin, C., 2003. Structural properties and photoreactivity relationships of substituted phenols in TiO_2 suspensions. Appl. Catal. B - Environ. 43, 293-301.

[14] Sharma, V.K., Zhao, J., Hidaka, H., 2014. Mechanism of photocatalytic oxidation of amino acids: Hammett correlations. Catal. Today. 224, 263-268.

[15] Ozen, A.S., Aviyente, V., 2004. Modeling the Substituent Effect on the Oxidative Degradation of Azo Dyes. J. Phys. Chem. A. 108, 5990-6000.

[16] Luo, J., Hu, J., Wei, X., Fu, L., Li, L., 2015. Dehalogenation of persistent halogenated organic compounds: A review of computational studies and quantitative structure-property relationships. Chemosphere. 131, 17-33.

[17] Bekbolet, M., Cınar, Z., Kılıç, M., Uyguner, C. S., Minero, C., Pelizzetti, E., 2009. Photocatalytic oxidation of dinitronaphthalenes: Theory and experiment. Chemosphere. 75, 1008-1014.

[18] Wang X., Chen J., Wang Y., Xie H., Fu Z., 2015. Transformation pathways of MeO-PBDEs catalyzed by active center of P450 enzymes: A DFT investigation employing 6-MeO-BDE-47 as a case. Chemosphere. 120, 631-636.

[19] Parr, R.G., Yang, W., 1989. Density-Functional Theory of Atoms and Molecules, Oxford University Press, Oxford.

[20] Bruzzone, S., Chiappe, C., Focardi, S.E., Pretti, C., Renzi, M., 2011. Theoretical descriptor for the correlation of aquatic toxicity of ionic liquids by quantitative structure-toxicity relationships. Chem. Eng. J. 175, 17-23.

[21] Redding, A.M., Cannon, F.S., Snyder, S.A., Vanderford, B.J., 2009. A QSAR-like analysis of the adsorption of endocrine disrupting compounds, pharmaceuticals, and personal care products on modified activated carbons. Water Res. 43, 3849-3861.

[22] Dostanić, J., Mijin, D., Uščumlić, G., Jovanović, D.M., Zlatar, M., Lončarević, D., 2014. Spectroscopic and quantum chemical investigations of substituent effects on the azo-hydrazone tautomerism and acid-base properties of arylazo pyridone dyes. Spectrochim. Acta A. 123, 37-45.

[23] Dostanić, J.M., Lončarević D.R., Banković P.T., Cvetković O.G., Jovanović D.M., Mijin D.Ž, 2011. Influence of process parameters on the photodegradation of synthesized azo

pyridone dye in TiO_2 water suspension under simulated sunlight. J. Environ. Sci. Health A: Tox. Hazard. Subst. Environ. Eng. 46, 70-79.

[24] Dostanić, J., Valentić, N., Uščumlić, G., Mijin, D., 2011. Synthesis of 5-(substituted phenylazo)-6-hydroxy-4-methyl-3-cyano-2-pyridones from ethyl 3-oxo-2-(substituted phenylazo)butanoate. J. Serb.Chem.Soc. 76 (4), 499-504.

[25] Gaussian 09, Revision C.01, M.J. Frisch, G.W. Trucks, H.B. Schlegel, G.E. Scuseria, M.A. Robb, J.R. Cheeseman, G. Scalmani, V. Barone, B. Mennucci, G.A. Petersson, H. Nakatsuji, M. Caricato, X. Li, H.P. Hratchian, A.F. Izmaylov, J. Bloino, G. Zheng, J.L. Sonnenberg, M. Hada, M. Ehara, K. Toyota, R. Fukuda, J. Hasegawa, M. Ishida, T. Nakajima, Y. Honda, O. Kitao, H. Nakai, T. Vreven, J.A. Montgomery, Jr., J.E. Peralta, F. Ogliaro, M. Bearpark, J.J. Heyd, E. Brothers, K.N. Kudin, V.N. Staroverov, R. Kobayashi, J. Normand, K. Raghavachari, A. Rendell, J.C. Burant, S.S. Iyengar, J. Tomasi, M. Cossi, N. Rega, J.M. Millam, M. Klene, J.E. Knox, J.B. Cross, V. Bakken, C. Adamo, J. Jaramillo, R. Gomperts, R.E. Stratmann, O. Yazyev, A.J. Austin, R. Cammi, C. Pomelli, J.W. Ochterski, R.L. Martin, K. Morokuma, V.G. Zakrzewski, G.A. Voth, P. Salvador, J.J. Dannenberg, S. Dapprich, A.D. Daniels, O. Farkas, J.B. Foresman, J.V. Ortiz, J. Cioslowski, D.J. Fox, Gaussian Inc, Wallingford CT, 2009.

[26] Zhao, Y., Truhlar, D.G., 2006. A new local density functional for main-group thermochemistry, transition metal bonding, thermochemical kinetics, and noncovalent interactions. J. Chem. Phys. 125 (19), 194101.

[27] Zhao, Y., Truhlar, D.G., 2008. The M06 suite of density functionals for main group thermochemistry, thermochemical kinetics, noncovalent interactions, excited states, and transition elements: two new functionals and systematic testing of four M06-class functionals and 12 other functionals. Theor. Chem. Acc. 120, 215-241.

[28] Hariharan, P.C., Pople, J.A., 1973. The influence of polarization functions on molecular orbital hydrogenation energies. Theor. Chim. Acta. 28, 213-222.

[29] Hirshfeld, F.L., 1977. Bonded-atom fragments for describing molecular charge densities. Theor. Chem. Acc. 44, 129-138.

[30] Reed A.E., Weinstock R.B., Weinhold F., 1985. Natural population analysis. J. Chem. Phys. 83, 735.

[31] Pearson, R.G., 1963. Hard and Soft Acids and Bases. J. Am. Chem. Soc. 85, 3533-3539.

[32] Gazquez, J. L., Mendez, F., 1994. The Hard and Soft Acids and Bases Principle: An Atoms in Molecules Viewpoint. J. Phys. Chem. 98, 4591-4593.

[33] Mendez, F., Gazquez, J. L. 1994. Chemical Reactivity of Enolate Ions: The Local Hard and Soft Acids and Bases Principle Viewpoint. J. Am. Chem. Soc. 116, 9298-9301.

[34] Yang, W., Mortier, W.J., 1986. The use of global and local molecular parameters for the analysis of the gas-phase basicity of amines. J. Am. Chem. Soc. 108, 5708-5711.

[35] Yang, W., Parr, R.G., 1985. Hardness, softness, and the fukui function in the electronic theory of metals and catalysis. Proc. Natl. Acad. Sci. USA, 82, 6723-6726.

[36] Johnson, C.D, 1973. The Hammett Equation, 1st ed. Cambridge University Press, Cambridge.

[37] Carey, F.A., Sundber, R.J., 2007. Advanced Organic Chemistry, 4th edition, Part A: structure and Mechanism, Chapter 4. Springer US, 389-473.

[38] Turchi, C.S., Ollis, D.F., 1990. Photocatalytic Degradation of Organic Water Contaminants: Mechanisms Involving Hydroxyl Radical Attack. J. Catal. 122, 178-192.

[39] Raman, M.S., Kesavan, M., Senthilkumar, K., Ponnuswamy, V., 2015. Ultrasonic, DFT and FT-IR studies on hydrogen bonding interactions in aqueous solutions of diethylene glycol. J. Mol. Liq. 202, 115-124.

[40] Yoosefian M., Mola A., 2015. Solvent effects on binding energy, stability order and hydrogen bonding of guanine-cytosine base pair. J. Mol. Liq. 209, 526-530.

[41] Ebead Y.H., 2011. Spectrophotometric investigations and computational calculations of prototropic tautomerism and acid-base properties of some new azo dyes. Dyes Pigments 92, 705-713.

[42] Rokhina E.V., Suri R.P.S., 2012. Application of density functional theory (DFT) to study the properties and degradation of natural estrogen hormones with chemical oxidizers. Sci. Total. Environ. 417-418, 280-290.

[43] Mendoza, L.H., 2014. A theoretical study of chemical reactivity of tartazine through DFT reactivity descriptors. J. Mex. Chem. Soc. 58, 416-423.

[44] Zhu, H., Shen, Z., Tang, Q., Ji, W., Jia, L., 2014. Degradation mechanism study of organic pollutants in ozonation process by QSAR analysis. Chem. Eng. J. 255, 431-436.

[45] Vos, A.M., Nulens, K.H.L., De Proft, F., Schoonheydt, R.A., Geerlings, P., 2002. Reactivity descriptors and rate constants for electrophilic aromatic substitution: acid zeolite catalyzed methylation of benzene and toluene. J. Phys. Chem. B 106, 2026-2034.

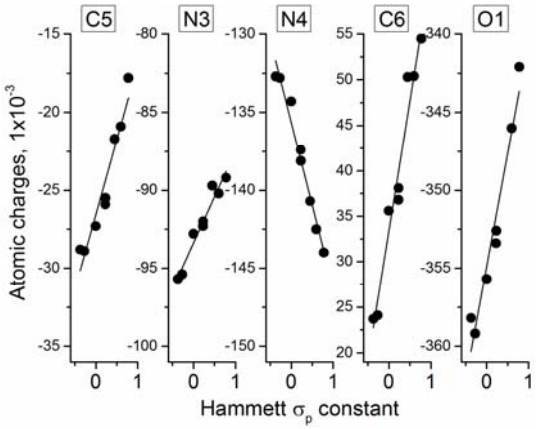

Fig. 1 Hirshfeld atomic charges of carbon atoms linked to azo bond (C5, C6), pyridone oxygen (O1) and azo nitrogen atoms (N3, N4) versus Hammett σ_p constant for the substituted arylazo pyridone dyes.

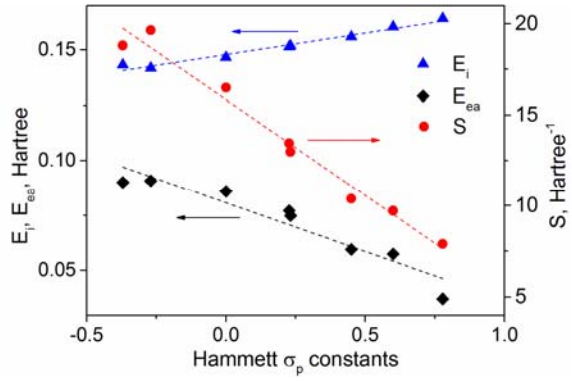

Fig. 2 Relation between global softness (S), ionisation energy (E_i), electron affinity (E_{ea}) and Hammett σ_p constant for the substituted arylazo pyridone dyes.

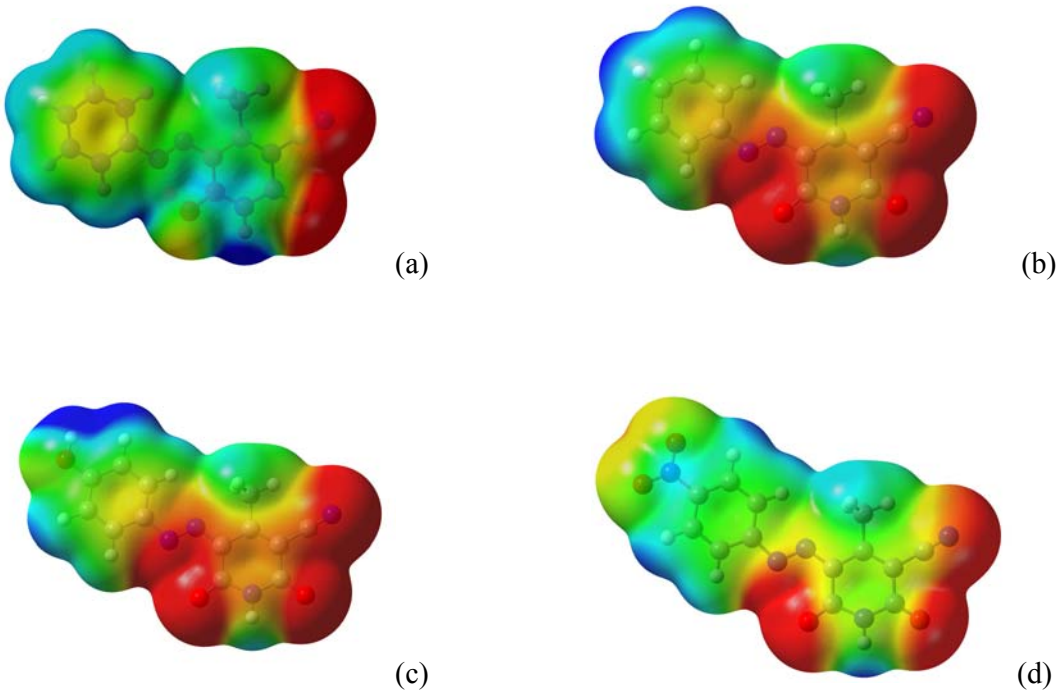

Fig. 3 The molecular electrostatic potential for neutral (a) R= H and anionic form (b) R=H, (c) R=OH, (d) R=NO_2 of substituted arylazo pyridone dye compounds. Potential decreases in the order blue > green > yellow > orange > red. (For interpretation of the references to colour in this Figure legend, the reader is referred to the web version of the article.)

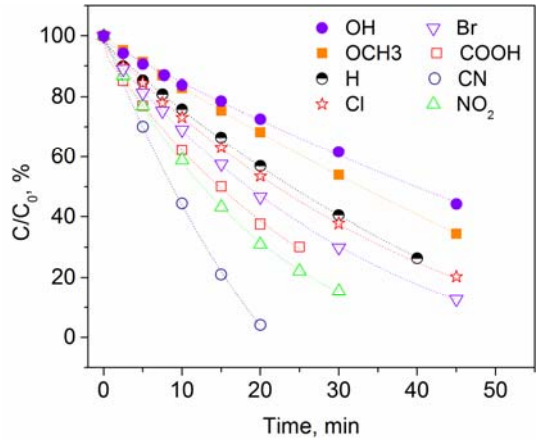

Fig. 4 Time-dependent photodegradation of aqueous solutions of substituted arylazo pyridone dyes (1×10^{-5} mol/dm^3). Solid symbols are referred to dyes with electron-donating substituents, while empty symbols are referred to dyes with electron-withdrawing substituents.

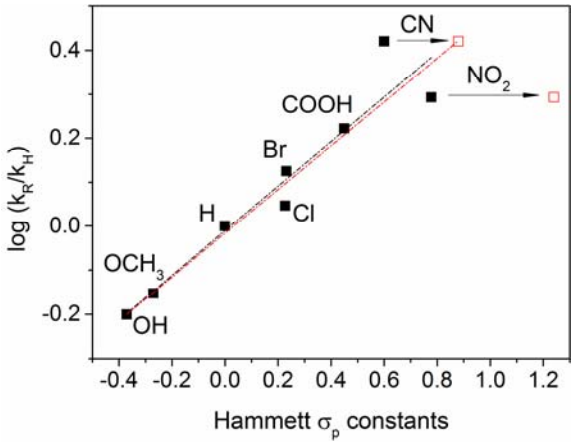

Fig. 5 The influence of substituent electronic effects on the apparent first-order rate constants of photocatalytic degradation of arylazo pyridone dyes. Solid symbols are referred to simple Hammett σ_p constants, while empty symbols are referred to σ^- constants.

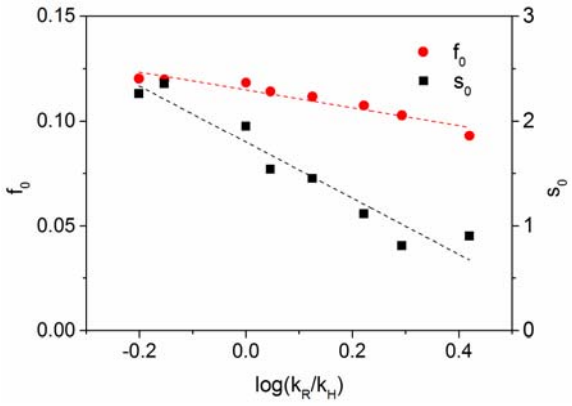

Fig. 6 Maximal radical Fukui functions (f_0) and local softness (s_0) calculated at M062X/6-31+G(d,p) level of theory and NPA atomic charges for the substituted arylazo pyridone dyes versus log (k_R/k_H).

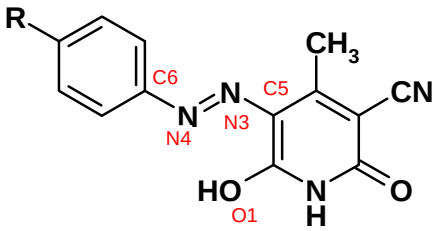

Scheme 1. Structure of studied 5-(4-substituted arylazo)-6-hydroxy-4-methyl-3-cyano-2-pyridones with added nuclei labels; R= OH, OCH_3, H, Cl, Br, COOH, CN, NO_2.

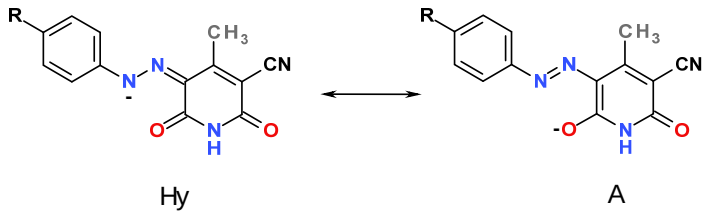

Scheme 2 Anionic form of arylazo pyridone dyes: "resonance hybrid" between azo anion (A) and hydrazone anion (Hy) canonical forms.

Table 1 Hirshfeld atomic charges and global softness (S) from M062X/6-31+G(d,p) calculations and determined kinetic parameters of photocatalytic degradation of substituted arylazo pyridone dyes.

Substituent, R	Hammett σ_p constants[a]	k_{app}[b] [min^{-1}]	log (k_R[c]/k_H[d])	Atomic charge					*S* [$Hartree^{-1}$]
				C5	N3	N4	C6	O1	
OH	-0.370	0.017	-0.201	-0.0288	-0.0957	-0.1327	0.0237	-0.3582	18.8060
OCH_3	-0.270	0.019	-0.153	-0.0289	-0.0954	-0.1328	0.0241	-0.3592	19.6451
H	0.000	0.027	0.000	-0.0273	-0.0928	-0.1343	0.0356	-0.3557	16.5006
Cl	0.227	0.030	0.046	-0.0259	-0.0923	-0.1374	0.0368	-0.3534	13.4643
Br	0.232	0.036	0.125	-0.0255	-0.0920	-0.1381	0.0381	-0.3526	12.9874
COOH	0.450	0.045	0.222	-0.0217	-0.0897	-0.1407	0.0503	-0.3242	10.3819
CN	0.600	0.071	0.420	-0.0209	-0.0902	-0.1425	0.0504	-0.3460	9.71810
NO_2	0.778	0.053	0.293	-0.0178	-0.0892	-0.1440	0.0545	-0.3421	7.88460

[a] the values are taken from Ref. [36],

[b] apparent first-order rate constant,

[c] apparent first-order rate constant of substituted dyes,

[d] apparent first order rate constant of unsubstituted dye.

Table 2 The condensed Fukui function (f_0) and local softness (s_0) for radical attack of azo nitrogen atoms (N3, N4) and carbon atoms linked to phenyl (C4) and pyridone ring (C5) of the substituted arylazo pyridone dyes calculated at M062X/6-31+G(d,p) level of theory and Hirshfeld atomic charges; Fukui function for OH radical=0.781; local softness for OH radical=1.550. Numbering system used throughout the calculations is shown in Scheme 1.

Substitu	f_0[a]				s_0[b]			
ent, R	C5	N3	N4	C6	C5	N3	N4	C6
OH	0.0529	0.0519	**0.0782**	0.0170	0.9954	0.9758	**1.4704**	0.3195
OCH3	0.0526	0.0522	**0.0774**	0.0162	1.0328	1.0253	**1.5196**	0.3177
H	0.0547	0.0522	**0.0771**	0.0179	0.9019	0.8609	**1.2716**	0.2954
Cl	0.0545	0.0505	**0.0742**	0.0186	0.7338	0.6806	**0.9994**	0.2510
Br	0.0543	0.0496	**0.0727**	0.0188	0.7055	0.6438	**0.9438**	0.2441
COOH	0.0413	0.0723	**0.0769**	0.0263	0.4294	0.7509	**0.7987**	0.2734
CN	0.0554	0.0451	**0.0632**	0.0232	0.5387	0.4379	**0.6137**	0.2255
NO_2	**0.0566**	0.0304	0.0460	0.0274	**0.4459**	0.2399	0.3626	0.2162

[a] condensed radical Fukui function,

[b] local softness.